EasyChair Preprint

№ 6045

A Nonlinear Fractional Partial Differential Equation for Image Denoising

Omar Gouasnouane, Noureddine Moussaid and Soumaya Boujena

July 11, 2021

A Nonlinear Fractional Partial Differential Equation for Image Denoising

1st Omar Gouasnouane
FST Mohammedia
Laboratory of Mathematics and Applications
PO Box 146, Mohammedia, Morocco
gouasnouane@gmail.com

2nd Noureddine Moussaid
FST Mohammedia
Laboratory of Mathematics and Applications
PO Box 146, Mohammedia, Morocco
noureddine.moussaid@fstm.ac.ma

3rd Soumaya Boujena
Ain-Chock Sciences Faculty
MACS Laboratory
Casablanca, Morocco
boujena@gmail.com

***Abstract*—The image denoising is a key step in image processing. This step can be treated by nonlinear diffusive filters requiring solving evolving partial differential equations. In this work we propose a nonlinear evolving partial differential equation with spatial fractional derivatives in order to improve the denoising capability and to extend some existing results in image denoising.**
The discretization of the fractional partial differential equation of the proposed model is performed using the shifted Grünwald-Letnikov formula useful for constructing stable numerical schemes.
The comparative analysis shows that the proposed model produces better or comparable quality of enhanced image than various well know and state of art techniques as well as several image analysis techniques.

***Index Terms*—image processing, image denoising, fractional order partial differential equation, nonlinear diffusion, fractional derivative**

I. Introduction

Noise is any undesired signal that contaminates the of brightness or color information in images. It can be arising from a variety of sources, including the discret nature of radiation, variation in detector sensitivity photographic grain effects, data tranmission errors, properties of imaging systems such as air turbuence or water droplets and image quantization errors.

Image denoising is an important research topic in image processing and computer vision. The goal of this step is to build an image from the avialable and which is as ideal as possible after eliminating the degradations undergone during the acquisition.

Several models for image denoising have been proposed in the literature, see [1], [2], [7]–[9], [19], [21]. Those models are based on linear and nonlinear diffusive filters requiring solving linear and nonlinear evolving partial differential equations (PDE).

Nonlinear diffusion filters are used in image processing to smooth out noisy images and enhance sharp contrasts in brightness simultaneously. This approach was initiated by P. Perona and J. Malik [19] by means of the following nonlinear PDE problem

$$\begin{cases} \dfrac{\partial v}{\partial t} - div(\mu(|\nabla v|)\nabla v) = 0, \ \text{ in } Q, \\ v(x,0) = v_0(x), \forall x \in \Omega, \\ \dfrac{\partial}{\partial \nu} v(x,t) = 0, \forall x \in \partial\Omega, \forall t \in [0,T], \end{cases} \tag{1}$$

where v_0 is the grey level distribution of a given (distored) image occupying a bounded domain Ω in $\mathbb{R}^d$ (with $d \leq 3$ in most applications) for which boundary is $\partial\Omega$. Q is defined by $Q = \Omega \times [0,T]$, for some given $T > 0$, and ν is the external vector normal to the domain boundary.

Starting from the initial image $v_0(x)$ and by running (1) we construct a family of functions (i.e images) $\{v(t,x)\}_{t>0}$ representing restored versions of $v_0(x)$. The diffusion coefficient $\mu(|\nabla v|)$ is designed such that:

- Inside the regions where the magnitude of the gradient of v is weak, equation (1) acts like the heat equation, resulting in isotropic smoothing.
- Near the boundaries where the magnitude of the gradient is large, the regularization is stopped and the edges are preserved.

The assumptions imposed on μ are usually

$$\begin{cases} \mu : [0,+\infty) \to [0,+\infty) \ \ decreasing, \\ \mu(0) = 1, \ \lim\limits_{s \to +\infty} \mu(s) = 0, \\ \mu(s) + 2s\mu'(s) > 0. \end{cases} \tag{2}$$

Typical examples for an edge stopping function μ which, in fact, have been used by Perona and Malik, are

$$\mu(s) = exp\left(-\frac{s^2}{k^2}\right) (k > 0). \tag{3}$$

$$\mu(s) = \frac{1}{1 + s^2/k^2} \ \ (k > 0). \tag{4}$$

The Parameter k is a measure for the steepness of an edge to be preserved.

The Perona-Malik model (1) and large amount of its modifications in the literature have demonstrated to be able to achieve a good compromis between noise removal and edge preservation. Unfortunately this model is ill-posed (see [15] for a proof of this in the one-dimensional context). Apart

of this inconvenient, numerical approximations of (1) do not exhibit significant instabilities. This numerical performance triggered many autheurs [1]–[3], [5]–[9], [20], to replace the Perona-Malik model by nearby versions which, on one hand side, admit solid analysis in terms of existence and uniqueness properties, and, on the other hand side, possess essentially the same numerical properties as (1). Although these models have been demonstrated to be able to achieve a good trade-off between noise removal and edge preservation.

Recentely, it has been demonstrated that many systems in many fields can be modeled more accurately by fractional order than integer order derivatives. It is well proved that as a fundamental mathematic tool, fractional order derivative shows great success in image processing [10].

In the last 40 years, fractional calculus began to shift from pure mathematics formulations to applications in various fields including biology, physics and mechanics amount to replace the classical derivativation in an evolution equation with a fractional order derivative. In particular in the image processing field [11]–[13], [16], the nonlocal properties of fractional differential models appear to give better results than traditional integral models.
In [12] Cuesta et al. proposed the equation

$$\frac{\partial^\alpha}{\partial t^\alpha}u(x,y,t) = \Delta u(x,y,t), \tag{5}$$

with $\dfrac{\partial^\alpha}{\partial t^\alpha}$ the Riemann-Liouville fractional time derivative of order $\alpha \in]1,2[$. This fractional order linear integro-differential equation interpolates a heat equation $(\alpha = 1)$ and a wave equation $(\alpha = 2)$.

In [4] Bai and Feng proposed a fractional order anisotropic diffusion equations, which are Euler-Lagrange equations of a cost functional which is an increasing function of the absolute value of the fractional derivative of the image intensity function. the proposed equations. It can be seen as generalizations of second-order and fourth-order anisotropic diffusion equations.

In [14], the authors proposed a fully fractional anisotropic diffusion equation which contains spatial as well as time fractional derivatives. It is a generalization of a method proposed by Cuesta [12] using time fractional derivatives, and the method proposed by Bai and Feng [4], which interpolates between the second and the fourth order anisotropic diffusion equation by the use of spatial fractional derivatives.

In this paper we attempt to extend the Perona-Malik's model by involving the fractional order derivatives with respect to the spatial variables using Grünwald-Letnikov fractional order derivative and the p-shifted Grünwald-Letnikov formula to implement the numerical scheme without using the discrete Fourier transfrom (DFT) which imposes the period boundary condition on the proposed equations.

Our algorithm is easy to implement compared to other algorithms that use discrete Fourier trasform in which an $m \times m$ input image is folded with respect to the lines $x = m - 1$ and $y = m - 1$ to produce an $2m \times 2m$ image to obtain a symmetric and continous borders of the original image but the size of the extended image requires additional memory and affects the computation cost and accuracy.

II. Fractional derivatives

The most known definitions of the fractional derivative are Grünwald-Letnikov, Riemann-Liouville, and Caputo, the first two are the most used in the field of image processing. The Grünwald-Letnikov definition is derived from the defintion of partial differential on integer order, while Riemann-Liouville, and Caputo definitions are derived from the integral order Cauchy formula.
The left and right Grünwald-Letnikov derivatives of order $\alpha > 0$ for a given function $f(x)$, $x \in [a,b]$ are defined by

$${}_{GL}D^\alpha_{a,x}f(x) = \lim_{\substack{h\to 0 \\ Nh=x-a}} \left(\frac{1}{h}\right)^\alpha \sum_{i=0}^{N}(-1)^\alpha \binom{\alpha}{i} f(x-ih), \tag{6}$$

and

$${}_{GL}D^\alpha_{x,b}f(x) = \lim_{\substack{h\to 0 \\ Nh=b-x}} \left(\frac{1}{h}\right)^\alpha \sum_{i=0}^{N}(-1)^\alpha \binom{\alpha}{i} f(x+ih), \tag{7}$$

respectively

The left and right Riemann-Liouville derivatives with order $\alpha > 0$ of the given function $f(x)$, $x \in [a,b]$ are defined as

$${}_{RL}D^\alpha_{a,x}f(x) = \frac{1}{\Gamma(n-\alpha)}\frac{d^n}{dt^n}\int_a^x \frac{1}{(x-s)^{\alpha+1-n}} f(s)ds,$$

and

$${}_{RL}D^\alpha_{x,b}f(x) = \frac{(-1)^n}{\Gamma(n-\alpha)}\frac{d^n}{dt^n}\int_x^b \frac{1}{(s-x)^{\alpha+1-n}} f(s)ds,$$

respectively, where Γ is the Euler's gamma function and n is a positive integer satisfying $n-1 \le \alpha \le n$.
If $f(x)$ is suitably smooth, i.e. $f \in \mathcal{C}^m[a,b]$ the Grünwald-Letnikov derivative of $f(x)$ and the Riemann-Liouville derivative of $f(x)$ are equivalent but in general the two definitions are not equivalent [10].

III. Nonlinear fractional order model

Our approach consists to extend the Perona-Malik (1) model by introducing the fractional order derivatives with respect to the spatial variables as follows,

$$\begin{cases} \dfrac{\partial u}{\partial t} - div^\alpha(\mu(|\nabla^\alpha u|)\nabla^\alpha u) = 0, \ \text{ in } Q, \\ u(x,0) = u_0(x), \forall x \in \Omega, \\ \dfrac{\partial u}{\partial \nu}(x,t) = 0, \forall x \in \partial\Omega, \forall t \in [0,T], \end{cases} \tag{8}$$

where the operators $div^{\alpha} = \dfrac{\partial^{\alpha}}{\partial x^{\alpha}} + \dfrac{\partial^{\alpha} u}{\partial y^{\alpha}}$ and $\nabla^{\alpha} = \left(\dfrac{\partial^{\alpha}}{\partial x^{\alpha}}, \dfrac{\partial^{\alpha}}{\partial y^{\alpha}}\right)$.

For numerical approximation of spatial fractional order derivatives we can use the formula derived from the Grünmald-Letnikov definition given by

$$\left({}_{GL}D^{\alpha}_{0,x} f(x)\right)_{x=x_k} \approx \left(\frac{1}{h}\right)^{\alpha} \sum_{i=0}^{k} \omega_i^{(\alpha)} f(x_k - ih)$$

where $\omega_i^{(\alpha)} = (-1)^i \binom{\alpha}{i}$ is the polynomial coefficients of $(1-z)^{\alpha}$, and can be calculate by the following recurrence formula

$$\begin{cases} \omega_0^{(\alpha)} = 1, \\ \forall i \in \{1, 2, ..., N\},\ \omega_i^{(\alpha)} = \left(1 - \dfrac{\alpha+1}{i}\right) \omega_{i-1}^{(\alpha)}. \end{cases} \tag{9}$$

The above approximatoin is convergent of order 1 for any $\alpha > 0$ [10].

This standard Grünwald-Letnikov formula may lead to unstable numerical schemes in solving fractional differential equations [10] for $1 < \alpha < 2$. To avoid this inconvinient the p-shifted Grünwald-Letnikov formula is useful for constructing stable numerical schemes.

The right shifted Grünwald-Letnikov formula is defined by

$$\left({}_{GL}D^{\alpha}_{a,x} f(x)\right)_{x=x_k} \approx \left(\frac{1}{h}\right)^{\alpha} \sum_{i=0}^{k+p} \omega_i^{(\alpha)} f(x - ih + p) \tag{10}$$

This shifted Grünwald-Letnikov formula gives a first order accuracy; the best performance comes from minimizing $|p - \alpha/2|$ [17], [18]. If $1 < \alpha \leq 2$, the optimal choice is $p = 1$. The case of $\alpha = 2$ reduces to the second order central difference method for the second order classical derivative.

To solve numerically the proposed model we begin with the fractional order gradient.

Let u be an image with $(n+1) \times (m+1)$ pixels. According to (10), the discrete fractional-order derivatives at the point (i, j) with the order α along the horizontal and the vertical direction, are respectively

$${}_{GL}D^{\alpha}_{x} u(i,j) = \left(\frac{1}{h}\right)^{\alpha} \sum_{k=0}^{k+p} \omega_i^{(\alpha)} u(k,j)\, \forall j \in \{0, 1, 2, ..., m\}. \tag{11}$$

And

$${}_{GL}D^{\alpha}_{y} u(i,j) = \left(\frac{1}{h}\right)^{\alpha} \sum_{k=0}^{k+p} \omega_i^{(\alpha)} u(i,k)\, \forall i \in \{0, 1, 2, ..., n\}. \tag{12}$$

Using the above formulas and by adobting the matrix form, the discretization of the fractional order gradient vector with α order is given, respectively for $j = 0, 1, 2, ..., m$ and for $i = 0, 1, 2, ..., n$ by

$$\begin{pmatrix} \frac{\partial^{\alpha}}{\partial x^{\alpha}} u_{0,j} \\ \frac{\partial^{\alpha}}{\partial x^{\alpha}} u_{1,j} \\ \frac{\partial^{\alpha}}{\partial x^{\alpha}} u_{2,j} \\ \vdots \\ \frac{\partial^{\alpha}}{\partial x^{\alpha}} u_{n-2,j} \\ \frac{\partial^{\alpha}}{\partial x^{\alpha}} u_{n-1,j} \\ \frac{\partial^{\alpha}}{\partial x^{\alpha}} u_{n,j} \end{pmatrix} = \left(\frac{1}{h}\right)^{\alpha} B_n^{(\alpha)} \begin{pmatrix} u_{0,j} \\ u_{1,j} \\ u_{2,j} \\ u_{3,j} \\ \vdots \\ u_{n-1,j} \\ u_{n,j} \end{pmatrix} \tag{13}$$

$$\begin{pmatrix} \frac{\partial^{\alpha}}{\partial y^{\alpha}} u_{i,0} \\ \frac{\partial^{\alpha}}{\partial y^{\alpha}} u_{i,1} \\ \frac{\partial^{\alpha}}{\partial y^{\alpha}} u_{i,2} \\ \vdots \\ \frac{\partial^{\alpha}}{\partial y^{\alpha}} u_{i,m-2} \\ \frac{\partial^{\alpha}}{\partial y^{\alpha}} u_{i,m-1} \\ \frac{\partial^{\alpha}}{\partial y^{\alpha}} u_{i,m} \end{pmatrix} = \left(\frac{1}{h}\right)^{\alpha} B_m^{\alpha} \begin{pmatrix} u_{i,0} \\ u_{i,1} \\ u_{i,2} \\ u_{i,3} \\ \vdots \\ u_{i,m-1} \\ u_{i,m} \end{pmatrix} \tag{14}$$

where $u_{i,j} = u(i,j)$ for $(i,j) \in \{0, 1, 2, ..., n\} \times \{0, 1, 2, ..., m\}$,

$$B_n^{(\alpha)} = \begin{pmatrix} \omega_1^{\alpha} & \omega_0^{\alpha} & 0 & 0 & 0 & \cdots & 0 \\ \omega_2^{\alpha} & \omega_1^{\alpha} & \omega_0^{\alpha} & 0 & 0 & \cdots & 0 \\ \omega_3^{\alpha} & \omega_2^{\alpha} & \omega_1^{\alpha} & \omega_0^{\alpha} & 0 & \cdots & 0 \\ \vdots & \ddots & \ddots & \ddots & \ddots & \ddots & \vdots \\ \omega_{n-2}^{\alpha} & \omega_{n-3}^{\alpha} & \cdots & \omega_2^{\alpha} & \omega_1^{\alpha} & \omega_0^{\alpha} & 0 \\ \omega_{n-1}^{\alpha} & \omega_{n-2}^{\alpha} & \omega_{n-3}^{\alpha} & \cdots & \omega_2^{\alpha} & \omega_1^{\alpha} & \omega_0^{\alpha} \\ \omega_n^{\alpha} & \omega_{n-1}^{\alpha} & \omega_{n-2}^{\alpha} & \omega_{n-3}^{\alpha} & \cdots & \omega_2^{\alpha} & \omega_1^{\alpha} \end{pmatrix}$$

and

$$B_m^{(\alpha)} = \begin{pmatrix} \omega_1^{\alpha} & \omega_0^{\alpha} & 0 & 0 & 0 & \cdots & 0 \\ \omega_2^{\alpha} & \omega_1^{\alpha} & \omega_0^{\alpha} & 0 & 0 & \cdots & 0 \\ \omega_3^{\alpha} & \omega_2^{\alpha} & \omega_1^{\alpha} & \omega_0^{\alpha} & 0 & \cdots & 0 \\ \vdots & \ddots & \ddots & \ddots & \ddots & \ddots & \vdots \\ \omega_{m-2}^{\alpha} & \omega_{m-3}^{\alpha} & \cdots & \omega_2^{\alpha} & \omega_1^{\alpha} & \omega_0^{\alpha} & 0 \\ \omega_{m-1}^{\alpha} & \omega_{m-2}^{\alpha} & \omega_{m-3}^{\alpha} & \cdots & \omega_2^{\alpha} & \omega_1^{\alpha} & \omega_0^{\alpha} \\ \omega_m^{\alpha} & \omega_{m-1}^{\alpha} & \omega_{m-2}^{\alpha} & \omega_{m-3}^{\alpha} & \cdots & \omega_2^{\alpha} & \omega_1^{\alpha} \end{pmatrix}.$$

We use a semi-discretizations in scale of the problem given by (1). We discretize the scaling interval $[0, T]$. Choosing $N \in \mathbb{N}$ we obtain the length of uniform discrete scale step $\Delta t = \frac{T}{N}$. The nonlinear terms of the equation are treated from the previous scale step while the linear terms are considered on the current scale level.

For every $k = 1, ...N$, we look for a function u^k, a solution of the equation

$$\frac{u^k - u^{k-1}}{\Delta t} - div^{\alpha}(\mu(\left|\nabla^{\alpha} u^{k-1}\right|) \nabla^{\alpha} u^{k-1}) = 0. \tag{15}$$

IV. Numerical experiments and interpretation

In this section, the performance of the proposed model will be compared with the classical Perona-Malik model [19] and the method proposed by Bai and al. [4], the selected RGB (truecolor) images includes 'toysflash' with size (650×420), 'peppers' with size (384×512).The Gaussian noise is added

to images with different variances values (0.001, 0.005, and 0.01). This noise is the most studied in the literature it occurs in practical situation.
The discret scaling step is selected to be $\Delta t = 1.E-2$ for boths models. We set the nonlinear diffusion coefficient $\mu(s) = 1/\sqrt{1+s^2}$. The values of the fractional order are taken with the range $\alpha \in]1, 2]$.

All testing problems were implemented using Matlab 2018a on Intel(R) Core(TM) i5 at 1.8GHz, 6GB memory, systeme type 64-bit and Windws 10 .
Four perfrmance metrics are considered here to evaluate the performance of restored image; peak signal to noise ratio (PSNR), signal to noise ratio (SNR), mean-squared error (MSE) and structural similarity index measure (SSIM).
The mean-squared error (MSE) between two images I_1 and I_2 is:

$$MSE = \frac{1}{n \times m} \sum_{n,m} \left(I_1(n,m) - I_2(n,m)\right)^2 \qquad (16)$$

n and m are the number of rows and columns in the input images, respectively.

$$SNR = 10 \times log_{10} \frac{\sum_{n,m} I_2^2}{\sum_{n,m} \left(I_1 - I_2\right)^2}, \qquad (17)$$

I_1 restored image and I_2 original image.

$$PSNR = 10 \times log_{10} \frac{R^2}{MSE}. \qquad (18)$$

R is the maximum fluctuation in the input image data type. For example, if the input image has a double-precision floating-point data type, then R is 1. If it has an 8-bit unsigned integer data type, R is 255, etc.

The Structural Similarity (SSIM) Index quality assessment index is used for measuring the similarity between two images.

$$SSIM = \frac{2\mu_x\mu_y + C1}{\mu_x^2 + \mu_y^2 + C1} \times \frac{2\sigma_{xy} + C2}{\sigma_x^2 + \sigma_y^2 + C2}, \qquad (19)$$

where μ_x, μ_y, σ_x, σ_y, and σ_{xy} are the means, standard deviations, and cross-covariance for images x, y. $C1$ and $C2$ denote constants used to maintain stability.

Figures 1 and 2 respectively show the comparison results of denoising images between the proposed model and the previously mentioned baseline methods.

The interpretation of the numerical simulations allows us to notice that our model has a good performance in visual quality, a lower mean square error (MSE), a higher value of peak signal-to-noise (PSNR) as well as for the rate of the signal-to-noise (SNR), and a better measure of the structural similarity index measure (SSIM) compared to those obtained by the previously mentioned baseline methods.

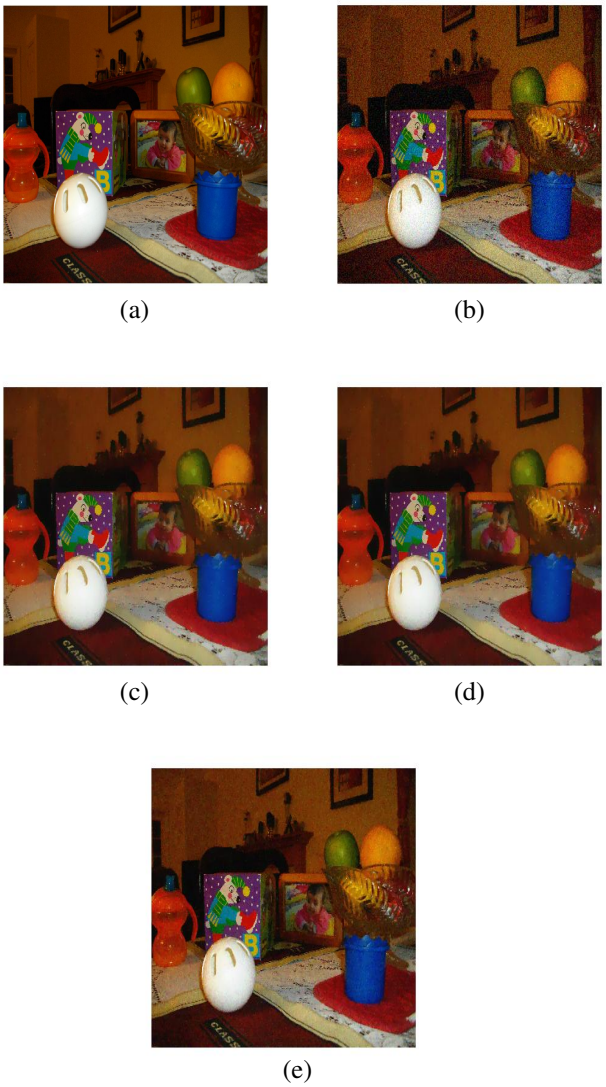

(a) (b) (c) (d) (e)

Fig. 1. Results corresponding to the toysflash image. (a) Clean image (650×420). (b) Noisy image affected by a Gaussian white noise with mean $m = 0$ and variance of 0.005, PSNR=23.83, SNR=14.63, MSE=268.72, SSIM=0.8. (c) Processed by the proposed model with $\alpha = 1.8$, PSNR=29.43, SNR=20.24, MSE=74.14, SSIM=0.924. (d) processed by the Perona-Malik model ($\alpha = 1$), PSNR=28.41, SNR=19.20, MSE=93.20, SSIM=0.909. (e) Processed by Bai and Feng model, PSNR=29.03, SNR=19.44, MSE=81.13, SSIM=0.913.

V. Conclusion

We propose, in this work, a fractional order nonlinear model for image denoising in which the spatial integer derivative in the classical Perona-Malik model is replaced with the spatial fractional order derivative. This new version can enhance the denoising capability. The interpretation of the numerical simulations allows us to notice that our model has a good performance in visual quality, a lower mean square error (MSE), a higher value of peak signal-to-noise (PSNR) as well as for the rate of the signal-to-noise (SNR), and a better measure of the structural similarity index measure (SSIM) compared to those obtained by other models.

Gaussian noise $m = 0$ and $\sigma = 0.005$				
α	PSNR	SNR	MSE	SSIM
1.2	27.93	17.97	128.85	0.803
1.4	28.86	18.63	97.42	0.875
1.6	29.01	19.78	81.13	0.913
1.8	29.43	20.24	74.14	0.924
2	28.97	19.71	97.51	0.907
Gaussian noise $m = 0$ and $\sigma = 0.01$				
α	PSNR	SNR	MSE	SSIM
1.2	25.21	18.20	112.59	0.873
1.4	26.45	19.02	98.90	0.896
1.6	27.12	19.51	97.85	0.901
1.8	27.45	19.68	94.53	0.912
2	26.89	19.45	98.87	0.896

TABLE I
PSNR, SNR, MSE AND SSIM FOR TOYSFLASH IMAGE WITH GAUSSIAN NOISE.

Gaussian noise $m = 0$ and $\sigma = 0.001$				
α	PSNR	SNR	MSE	SSIM
1.2	30.93	23.54	32.74	0.816
1.4	33.79	25.94	26.18	0.945
1.6	34.02	26.12	24.03	0.975
1.8	34.41	26.43	23.52	0.980
2	33.97	26.07	25.38	0.971
Gaussian noise $m = 0$ and $\sigma = 0.01$				
α	PSNR	SNR	MSE	SSIM
1.2	26.96	18.13	124.67	0.887
1.4	27.11	18.85	119.53	0.901
1.6	27.34	19.23	112.13	0.937
1.8	27.71	19.74	109.93	0.940
2	27.07	19.12	114.42	0.913

TABLE II
PSNR, SNR, MSE AND SSIM FOR PEPPERS IMAGE WITH GAUSSIAN NOISE.

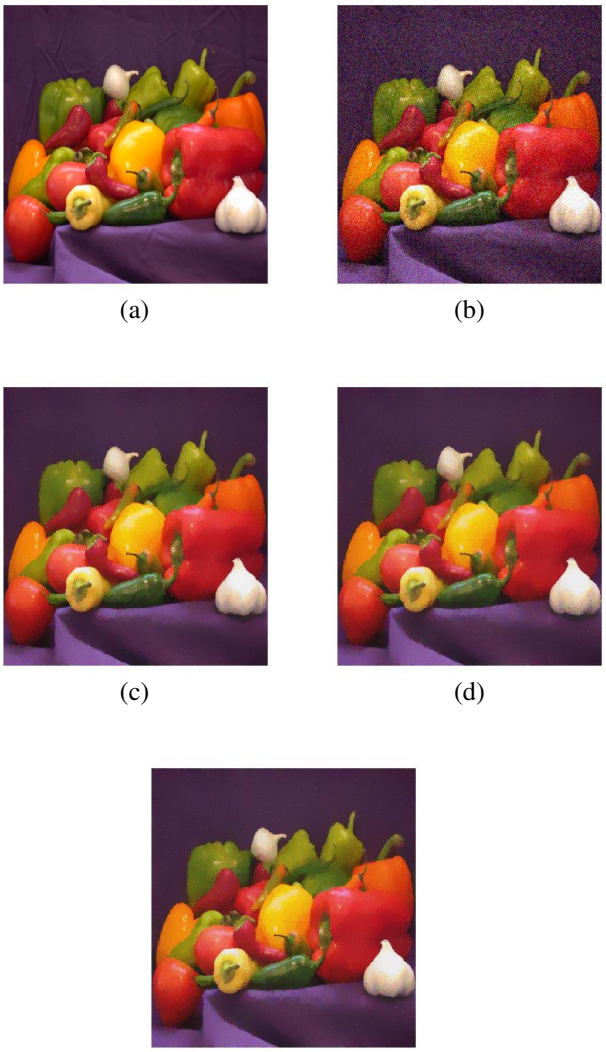

Fig. 2. Results corresponding to the peppers image. (a) Clean image (650×420). (b) Noisy image affected by a Gaussian white noise with mean $m = 0$ and variance of 0.01, PSNR=20.46, SNR=12.4, MSE=583.66, SSIM=0.647. (c) Processed by the proposed model with $\alpha = 1.8$, PSNR=27.71, SNR=19.74, MSE=109.93, SSIM=0.940. (d) processed by the Perona-Malik model ($\alpha = 1$), PSNR=26.43, SNR=18.45, MSE=147.85, SSIM=0.925. (e) Processed by Bai and Feng model, PSNR=27.10, SNR=19.12, MSE=126.72, SSIM=0.931.

REFERENCES

[1] R. Aboulaich, S. Boujena, and E. EL Guarmah, "A Nonlinear Parabolic Model in Processing of Medical Image", Math. Model. Nat. Phenom., vol. 3, no. 6, pp. 131–145, 2008.

[2] R. Aboulaich, S. Boujena, and E. EL Guarmah, "Sur un modèle non-linéaire pour le débruitage de l'image", C.R. Acad. Sci. Paris. Ser. I, vol. 345, pp. 425–429, 2007.

[3] L. Alvarez, P. L. Lions, and J. M. Morel, "Image selective smoothing and edge detection by nonlinear diffusion", SIAM J. Numer. Anal., vol. 29, no. 3, pp. 845–866, 1992.

[4] J. Bai and X. Feng, "Fractional-Order Anisotropic Diffusion for Image Denoising", IEEE Transactions on Image Processing, vol. 16, no. 10, pp. 2492–2502, 2007.

[5] S. Boujena, E. EL Guarmah, O. Guasnouane, and J. Pousin, "An Improved Nonlinear Model for Image Restoration", Pure and Applied Functional , vol. 2, no. 4, pp. 599–623, 2017.

[6] S. Boujena, E. EL Guarmah, O. Guasnouane, and J. Pousin, "On a derived non linear model in image restoration", Proceedings of 2013 International Conference on Industrial Engineering and Systems Management (IESM), pp. 1–3, 2013.

[7] S. Boujena, K. Bellaj, O. Gouasnouane, and E. El Guarmah, "An improved nonlinear model for image inpainting", Applied Mathematical Sciences, vol. 9, no. 124, pp. 6189–6205, 2015.

[8] S. Boujena, K. Bellaj, O. Gouasnouane, and E. El Guarmah, "One approach for image denoising based on finite element method and domain decomposition technique", International Journal of Applied Physics and Mathematics (IJAPM), vol. 7, no. 2, pp. 141–147, 2017.

[9] F. Catté, P. L. Lions, J.M. Morel and T. Coll, "Image selective smoothing and edge detection by a nonlinear", SIAM Journal on Numerical Analysis, vol. 29, no. 1, pp. 182–193, 1992.

[10] L. Changpin, Z. Fanhai, "Numerical Methods for Fractional Calculus", Published May 19th 2015 by CRC Press.

[11] D. Chen, Y. Chen and D. Xue, "1-D and 2-D digital fractional-order savitzky-golay differentiator", Signal, Image and Video Processing, vol. 6, no. 3, pp. 503–511, 2012.

[12] E. Cuesta and J. Codes, "Image processing by means of a linear integro-differential equation", in 3rd IASTED Int. Conf. Visualization, Imaging and Image Processing, vol. 1, pp. 438–442, 2003.

[13] S. Didasa, B. Burgeth, A. Imiya and J. Weickert, "Regularity and scalespace properties of fractional high order linear filtering", Scale Spaces and PDE Methods in Computer Vision, pp. 13–25, 2005.

[14] M. Janev, S. Pilipovic, T. Atanackovic, R. Obradovic, N. Ralevic, "Fully fractional anisotropic diffusion for image denoising", Mathematical and Computer Modelling, vol. 54, no. 1-2, pp. 729–741, 2011.

[15] S. Kichenassamy, "The Perona-Malik paradox", SIAM J. APPL. MATH., vol. 57, no. 5, pp. 1328–1342, 1997.

[16] H. Li, Z. Yu and C. Mao, "Fractional differential and variational method for image fusion and super-resolution", Neurocomputing, vol. 171, pp.

138–148, 2016.
[17] M. Meerschaert and C. Tadjeran, “Finite difference approximations for fractional advection-dispersion flow equations“, J. Comput. Appl. Math., vol. 172, pp. 65–77, 2004.
[18] K. Oldham and J. Spanier, “The Fractional Calculus“. Academic Press, New York, 1974.
[19] P. Perona and J. Malik, “Scale-espace and edge detection using anisotropic diffusion“, IEEE Transaction on Pattern Analysis and Machine Intelligence, vol. 12, pp. 429–439, 1990.
[20] J. Weickert, “Anisotropic Diffusion in Image Processing“, PhD thesis, University of Kaiserslautern, Germany, Laboratory of Technomathematics. January 1996.
[21] J. Weickert, M. Bart, H. Romeny ter and A. Viergever Max, “Efficient and reliable Schemes for nonlinear Diffusion Filtering“, IEEE Trans., Image Processing, vol. 7, no. 3, pp. 398–410, 1998.